Photosynthesis Research (2018) 136:315–328
https://doi.org/10.1007/s11120-017-0466-8

ORIGINAL ARTICLE

# Anatomical and diffusional determinants inside leaves explain the difference in photosynthetic capacity between *Cypripedium* and *Paphiopedilum*, Orchidaceae

**Zhong-Hui Yang[1,2,3] · Wei Huang[1,2] · Qiu-Yun Yang[1,2] · Wei Chang[1,2] · Shi-Bao Zhang[1,2]**

Received: 19 April 2017 / Accepted: 16 November 2017 / Published online: 20 November 2017


## Abstract

Comparing with other angiosperms, most members within the family Orchidaceae have lower photosynthetic capacities. However, the underlying mechanisms remain unclear. *Cypripedium* and *Paphiopedilum* are closely related phylogenetically in Orchidaceae, but their photosynthetic performances are different. We explored the roles of internal anatomy and diffusional conductance in determining photosynthesis in three *Cypripedium* and three *Paphiopedilum* species, and quantitatively analyzed their diffusional and biochemical limitations to photosynthesis. *Paphiopedilum* species showed lower light-saturated photosynthetic rate ($A_N$), stomatal conductance ($g_s$), and mesophyll conductance ($g_m$) than *Cypripedium* species. $A_N$ was positively correlated with $g_s$ and $g_m$. And yet, in both species $A_N$ was more strongly limited by $g_m$ than by biochemical factors or $g_s$. The greater $g_s$ of *Cypripedium* was mainly affected by larger stomatal apparatus area and smaller pore depth, while the less $g_m$ of *Paphiopedilum* was determined by the reduced surface area of mesophyll cells and chloroplasts exposed to intercellular airspace per unit of leaf area, and much thicker cell wall thickness. These results suggest that leaf anatomical structure is the key factor affecting $g_m$, which is largely responsible for the difference in photosynthetic capacity between those two genera. Our findings provide new insight into the photosynthetic physiology and functional diversification of orchids.

**Keywords** Leaf anatomy · Mesophyll conductance · Orchidaceae · Photosynthetic limitations · Stomatal conductance

## Abbreviations

| | |
|---|---|
| $A_N$ | Light-saturated net rate of $CO_2$ assimilation at 380 μmol mol$^{-1}$ $CO_2$ concentration (20 °C for *Cypripedium* and 25 °C for *Paphiopedilum*) (μmol $CO_2$ m$^{-2}$ s$^{-1}$) |
| $A_s$ | Area of individual stomata (μm$^2$) |
| $A_{sc}$ | Area of intercellular airspace in the substomatal cavity (μm$^2$) |
| $C_a$ | Ambient $CO_2$ concentration (μmol mol$^{-1}$) |
| $C_c$ | Chloroplast $CO_2$ concentration (μmol mol$^{-1}$) |
| $C_i$ | $CO_2$ concentration in substomatal cavities (μmol mol$^{-1}$) |
| $CT_{ab}$ | Abaxial cuticle thicknesses (μm) |
| $CT_{ad}$ | Adaxial cuticle thickness (μm) |
| $C_{transition}$ | Chloroplast $CO_2$ concentration at which the transition from Rubisco to RuBP regeneration limitation occurs |
| $ET_{ab}$ | Abaxial epidermis thickness (μm) |
| $ET_{ad}$ | Adaxial epidermis thickness (μm) |
| ETR | Rate of linear electron transport in photochemistry at $A_N$ (μmol electron m$^{-2}$ s$^{-1}$) |
| $f_{ias}$ | Intercellular airspace as a percentage of leaf volume (%) |
| $g_m$ | Mesophyll conductance (mol $CO_2$ m$^{-2}$ s$^{-1}$) |
| $g_s$ | Stomatal conductance (mol $CO_2$ m$^{-2}$ s$^{-1}$) |
| $g_{tot}$ | Total conductance (mol $CO_2$ m$^{-2}$ s$^{-1}$) |
| $J_{max}$ | Maximum rate of electron transport (μmol electron m$^{-2}$ s$^{-1}$) |
| $K_c$ | Michaelis–Menten constants for $CO_2$ (μmol mol$^{-1}$) |

**Electronic supplementary material** The online version of this article (https://doi.org/10.1007/s11120-017-0466-8) contains supplementary material, which is available to authorized users.

✉ Shi-Bao Zhang
sbzhang@mail.kib.ac.cn

[1] Key Laboratory of Economic Plants and Biotechnology, Kunming Institute of Botany, Chinese Academy of Sciences, Kunming 650201, China

[2] Yunnan Key Laboratory for Wild Plant Resources, Kunming 650201, Yunnan, China

[3] University of Chinese Academy of Sciences, Beijing 100049, China

| | |
|---|---|
| $K_o$ | Michaelis–Menten constants for $O_2$ (mmol $mol^{-1}$) |
| $L_b$ | Biochemical limitation of photosynthesis (%) |
| $L_c$ | Total length of chloroplast perimeter facing the intercellular airspace (μm $m^{-2}$) |
| LMA | Leaf dry mass per unit area (g $m^{-2}$) |
| $L_{mc}$ | Mesophyll conductance limitation (%) |
| $L_{mes}$ | Total length of mesophyll cell perimeter facing the intercellular airspace (μm $m^{-2}$) |
| $L_s$ | Stomatal limitation (%) |
| LT | Leaf thickness (μm) |
| MT | Mesophyll layer thickness (μm) |
| $N_{area}$ | Leaf nitrogen content per unit area (g $m^{-2}$) |
| $N_{mass}$ | Leaf nitrogen content per unit dry mass (%) |
| $O$ | Intercellular $O_2$ concentration (mmol $mol^{-1}$) |
| PD | Pore depth (μm) |
| PNUE | Photosynthetic nitrogen use efficiency (μmol $s^{-1}$ $CO_2$ mmol $g^{-1}$ N) |
| $R_d$ | Rate of mitochondrial respiration measured in the dark (μmol $CO_2$ $m^{-2}$ $s^{-1}$) |
| RH | Relative humidity (%) |
| SA | Stomatal aperture area ($\mu m^2$) |
| $S_{c/o}$ | In vitro Rubisco specificity factor |
| $S_c/S$ | Chloroplast surface area exposed to intercellular airspace per unit of leaf area ($m^2$ $m^{-2}$) |
| $S_c/S_{mes}$ | Proportion of exposed chloroplast to mesophyll surface areas ($m^2$ $m^{-2}$) |
| SCD | Substomatal cavity depth (μm) |
| SD | Stomatal density ($mm^{-2}$) |
| SL | Stomatal length (μm) |
| $S_{mes}/S$ | Mesophyll surface area exposed to intercellular airspace per unit leaf area ($m^2$ $m^{-2}$) |
| $S_s$ | Cross-sectional areas for mesophyll cells ($m^2$ $m^{-2}$) |
| SW | Stomatal width (μm) |
| $T_{chlor}$ | Chloroplast thickness (μm) |
| $T_{cw}$ | Cell wall thickness (μm) |
| $V_{c,max}$ | Maximum rate of carboxylation (μmol $CO_2$ $m^{-2}$ $s^{-1}$) |
| $V_{o,max}$ | Maximum RuBP saturated rate of oxygenation (μmol $O_2$ $m^{-2}$ $s^{-1}$) |
| VPD | Vapor pressure deficit (kPa) |
| $W$ | Width of leaf section (μm) |
| $\Gamma^*$ | $CO_2$ concentration at which net $CO_2$ fixation offsets $CO_2$ loss from photorespiration (μmol $mol^{-1}$) |

## Introduction

The Orchidaceae is one of the largest and most diverse families of flowering plants. With approximately 28,000 species spanning 736 genera, this family is widely distributed in various ecosystems throughout the world, except at the two Poles and in desert regions (Dressler 1993; Christenhusz and Byng 2016). However, because of their great economic importance to floral and pharmaceutical industries, as well as recent habitat losses, many of those species are now only locally distributed and becoming rare (Crain and Tremblay 2014). The photosynthetic potential is lower for most members of this family than for other angiosperm species (Assmann and Zeiger 1985; Hew and Yong 2004; Moreira et al. 2009; Zhang et al. 2015). Orchid plants usually grow slowly and have a long vegetative period (Shefferson 2006). This slower growth might be attributed to their reduced photosynthetic capacity (Obeso 2002). Although this low potential in some orchids might be due to crassulacean acid metabolism (Kerbauy et al. 2012), some $C_3$ orchids also have this characteristic (Assmann and Zeiger 1985; Zhang et al. 2015). Therefore, the reasons for the low photosynthetic efficiencies in orchids remain unclear, especially our understanding of the correlation between leaf internal structure and photosynthetic capacity.

Although both *Cypripedium* and *Paphiopedilum* belong to the diandrous orchid subfamily Cypripedioideae (Cox et al. 1997; Cameron et al. 1999) and are closely related phylogenetically (Cox et al. 1997), the photosynthetic capacity of species in the former is approximately three to four times greater than that of species in the latter (Zhang et al. 2010; Chang et al. 2011). Both genera also have obvious differences in their leaf characters and geographical distribution. *Cypripedium* is a genus with ~50 species; they are perennial geophytes which are dormant in the winter. China is the main distribution area with 32 species and one variant at altitudes of above 1800 m in southwest China, including 24 endemic species. These species usually grow in humus-rich soils with good properties for absorbing and holding water in alpine grasslands, subalpine woodlands, and understory areas. However, *Paphiopedilum* are evergreen plants; there are 66 species, with 27 known species in China. Most of these species grow in karst limestone areas below an altitude of 2000 m with relatively poor soil and low water availability (Guan et al. 2011; Zhang et al. 2012). Therefore, these wide contrasts in morphology and photosynthesis, accompanied by their close relatedness, make *Cypripedium* and *Paphiopedilum* a valuable system for exploring the association of leaf structure with photosynthetic capacity in Cypripedioideae.

Investigating leaf morphology and anatomy is crucial to understanding why Orchidaceae often has such low photosynthetic potential, because those traits somewhat affect plant resource acquisition, gas diffusional resistance, physiological functions, and adaptations to environmental changes (Holbrook and Putz 1996). Leaf photosynthesis is determined by the concentration of $CO_2$ inside the photosynthetic carboxylation sites and by the efficiency of plants to assimilate $CO_2$ (Evans and von Caemmerer 1996; Muir

et al. 2014). However, before atmospheric $CO_2$ arrives at the carboxylation site, it must pass through a series of 'physical barriers', including the stomata, intercellular airspaces, cell walls, plasma membrane, cytosol, and chloroplast envelopes and stroma (Evans and von Caemmerer 1996; Flexas et al. 2012; Tomas et al. 2013; Muir et al. 2014). Hence, net $CO_2$ assimilation is directly affected by $CO_2$ diffusion resistance from ambient air to carboxylation sites in the chloroplasts (Farquhar and Sharkey 1982; Ball et al. 1987; Peguero-Pina et al. 2012). It is possible that the low photosynthetic rate found with Orchidaceae may be attributed to diffusional limitations that involve stomatal conductance ($g_s$, the conductance of $CO_2$ from the atmospheric environment into stomata) and mesophyll conductance ($g_m$, the conductance of $CO_2$ from the substomatal cavity to the carboxylation sites) to $CO_2$ (Grassi and Magnani 2005; Gago et al. 2013). See the list of all abbreviations provided at the beginning of the paper. At each step in the diffusion pathway, leaf morphology and anatomy impact $CO_2$ conductance (Flexas et al. 2006; Niinemets and Sack 2006; Muir et al. 2014). Because stomata represent important channels for this diffusion into the leaf, the pattern of stomatal distribution on the abaxial and adaxial leaf surfaces as well as stomatal density, aperture, and size are key anatomical traits that influence $g_s$ (Franks and Beerling 2009; Giuliani et al. 2013). For example, the unique stomatal structure and lack of chloroplasts in the guard cells can limit stomatal opening in *Paphiopedilum*, resulting in low photosynthetic performance (Zhang et al. 2010). Stomatal conductance is also correlated with leaf morphological traits, including leaf density (as leaf dry mass per unit area divided by leaf thickness) and thickness, leaf area, and abaxial and adaxial epidermis thicknesses (Dunbar-Co et al. 2009; Zhang et al. 2010, 2012). One potential strategy for improving performance is to increase stomatal density and reduce pore size because smaller stomata have greater sensitivity to environmental change (Franks and Farquhar 2007). Although researchers already recognize that orchids have lower stomatal density and larger stomata than other angiosperms (Guan et al. 2011; Zhang et al. 2015), it is still unclear how those traits affect photosynthesis in orchids.

The role that mesophyll conductance has in photosynthesis is a new focus of research that has produced results suggesting that $g_m$ is finite and variable, and is a major limiting factor (Grassi and Magnani 2005; Niinemets et al. 2005, 2009; Muir et al. 2014; Gago et al. 2016; Han et al. 2016). Resistance to mesophyll diffusion due to specific anatomical structures can be quantified in terms of leaf dry mass per unit area, leaf thickness, leaf density, surface area of the mesophyll cells exposed to intercellular airspace per unit of leaf area, and the fraction of the mesophyll occupied by intercellular airspace (Oguchi et al. 2003; Peguero-Pina et al. 2012; Tosens et al. 2012). However, the most powerful sources of $g_m$ variation are the amount of chloroplast surface area exposed to intercellular airspace per unit of leaf area and the cell wall thickness (Tholen and Zhu 2011; Carriqui et al. 2015; Tosens et al. 2016). This influence of leaf anatomy on $g_m$ differs by species (Flexas et al. 2014), but the impact of such anatomical parameters on $g_m$ and photosynthesis has rarely been tested in orchids.

Photosynthetic capacity can also be affected by biochemical factors, such as leaf N content, Rubisco activity, and N-partitioning into photosynthetic components. Being widely distributed in organelles that have photosynthetic functioning, Rubisco is the most abundant naturally occurring protein on earth. Consequently, it can directly affect net photosynthetic production, and its content and activity can modulate the rate of $CO_2$ assimilation in plants (Sawada et al. 2003; Yamori et al. 2012). Nitrogen is an important raw material for chlorophyll and carboxylase, and leaf photosynthesis in numerous plants, including eucalyptus and orchid, is closely related to their leaf N contents (Laclau et al. 2004; Yamori et al. 2011).

Leaf photosynthetic performance is generally regulated through a combination of stomatal, mesophyll, and biochemical limitations (Grassi and Magnani 2005; Flexas et al. 2012; Tomas et al. 2013). For example, the biochemical limitation ($L_b$) is the largest factor depressing photosynthesis in seven angiosperms and eight wild relatives of *Solanum* sect. *Lycopersicon*, followed by mesophyll conductance ($L_{mc}$) and stomatal ($L_s$) limitations, while $L_{mc}$ is the most important factor controlling fern photosynthesis, followed by $L_s$ and $L_b$ (Muir et al. 2014; Carriqui et al. 2015). Those findings indicate that the extent to which biochemical and diffusional factors affect photosynthetic performance varies across species (Terashima et al. 2006; Flexas et al. 2008, 2012). Despite these scientific advances, however, no investigations have been reported on the relative contribution of those three types of limitations to the low photosynthetic capacity of orchids.

We selected six closely related $C_3$ orchid species (three each from *Cypripedium* and *Paphiopedilum*) and compared their rates of photosynthesis, as well as key anatomical and physiological traits. Our main objectives were to improve our understanding of (1) how leaf anatomical structures affect stomatal and mesophyll conductance and photosynthetic performances and (2) the relative roles of stomatal, mesophyll, and biochemical limitations to orchid photosynthesis.

## Materials and methods

### Plant materials and growing conditions

We investigated the association between photosynthesis and orchid leaf anatomy, diffusional resistance, and biochemistry, using three *Cypripedium* species (*C. flavum, C.*

*tibeticum*, and *C. yunnanense*) and three *Paphiopedilum* species (*P. armeniacum, P. micranthum*, and *P. dianthum*). The photosynthetic type of these six selected species is $C_3$ photosynthesis (Guan 2010). The aim of selecting those closely related species was to alleviate the effect of large morphological and physiological differences caused by phylogeny (Peguero-Pina et al. 2017). The ecological, habitat, and leaf characteristics of the six species are shown in Appendix S1. Because the optimal growth conditions are different between *Paphiopedilum* and *Cypripedium* (Guan et al. 2010; Chang et al. 2010), they were cultivated at two sites to ensure their best growth and physiological performances. The *Paphiopedilum* species were grown in a greenhouse in Kunming Botanical Garden (elevation 1990 m; 102°410′E, 25°01′N). The growth conditions included an air temperature of 20–25 °C (day) and 10–15 °C (night), 70–80% of relative humidity (RH), and with a maximum mid-day PPFD of approximately 800 µmol photons $m^{-2}$ $s^{-1}$. The three *Cypripedium* species were grown in Shangrila Alpine Botanical Garden (elevation 3260 m; 99°50′E, 27°48′N) with a temperature of 15–23 °C at day and approximately 10 °C at night, and RH ranging from 60 to 85% during the growing period. The maximum light intensity received by the plants was approximately 1000 µmol photons $m^{-2}$ $s^{-1}$. All sampling and measurements were conducted during their respective flowering periods in 2016, i.e., *Paphiopedilum* in September and *Cypripedium* in June.

## Monitoring of photosynthetic gas exchange

All measurements of leaf gas exchange were performed on clear days by clamping fully expanded and healthy leaves from each species into 2-$cm^2$ cuvettes in an open infrared gas exchange system with an integrated fluorescence chamber (LI-6400-40; Li-Cor, Lincoln, NE, USA). To ensure that the results from these two genera would be comparable, mature leaves (the species of *Cypripedium* at a leaf age of 60 days and *Paphiopedilum* at a leaf age of 2 years) were used for photosynthetic measurements under the optimum conditions established previously (Chang et al. 2011; Zhang et al. 2006). For photosynthetic measurements, RH was maintained at approximately 60%, vapor pressure deficit (VPD) at approximately 1.5 kPa, and leaf temperatures at 25 °C for *Paphiopedilum* and 20 °C for *Cypripedium* (see Guan et al. 2011; Chang et al. 2011 for temperatures used in previous studies). The leaf steady-state conditions of these two genera were induced for 25–30 min prior to the measurement period, using a chamber $CO_2$ concentration of 380 µmol $mol^{-1}$ and a saturating photosynthetic photon flux density of 400 µmol photons $m^{-2}$ $s^{-1}$ for *Paphiopedilum* and 800 µmol photons $m^{-2}$ $s^{-1}$ for *Cypripedium*.

Photosynthetic $CO_2$ response curves were tested with $CO_2$ concentrations ranging from 0 to 2000 µmol $mol^{-1}$. The automatic protocol system for the LI-6400-40 was used to maintain a light intensity of 400 µmol photons $m^{-2}$ $s^{-1}$ for *Paphiopedilum* and 1200 µmol photons $m^{-2}$ $s^{-1}$ for *Cypripedium* (Zhang et al. 2006; Guan et al. 2011; Chang et al. 2011). Photosynthetic rates and chlorophyll fluorescence were recorded within a steady state by setting the wait time of each concentration at 3 min. Five leaves per species were sampled from different plants.

The photosynthetic response curves for $CO_2$ were fitted by Photosyn Assistant software V1.1 (Dundee Scientific, UK), and the maximum rate of carboxylation ($V_{c,max}$) was determined as described by Long and Bernacchi (2003). Using the $A_N$–$C_i$ curves, mesophyll conductance was calculated according to the method of Harley et al. (1992):

$$g_m = \frac{A_N}{C_i - \Gamma^*\left[ETR + 8\left(A_N + R_d\right)\right] / \left[ETR - 4\left(A_N + R_d\right)\right]},$$

where $A_N$, $C_i$, and ETR are the net photosynthetic rate, the $CO_2$ concentration in substomatal cavities, and the rate of electron transport at the ambient $CO_2$ concentration, respectively. Synchronized with the measurement of photosynthetic $CO_2$ response curve, the value of ETR was determined by a portable photosynthesis analysis system with a LI-6400-40 fluorescence chamber. $R_d$ is the dark respiration rate and was measured after 30-min dark adaptation at daytime. The $CO_2$ concentration at which net $CO_2$ fixation offsets $CO_2$ loss from photorespiration ($\Gamma^*$) was calculated from Rubisco specificity factor at a temperature of 20 °C in *Cypripedium* species and 25 °C in *Paphiopedilum* using the following equation (von Caemmerer 2000; Sharkey et al. 2007):

$$\Gamma^* = \frac{0.5 \cdot \left[O_2\right]}{S_{c/o}},$$

where $S_{c/o}$, the Rubisco specificity factor, was derived from Rubisco kinetics as

$$S_{c/o} = \frac{V_{c,max} K_o}{V_{o,max} K_c},$$

where $V_{o,max}$, the maximum RuBP saturated rate of oxygenation, equals 1/2 $V_{c,max}$. $K_c$ and $K_o$ are Michaelis constants for $CO_2$ and $O_2$, respectively. Because $K_o$ and $K_c$ are temperature dependent, their values at given temperatures for each species (20 °C for *Cypripedium* species and 25 °C for *Paphiopedilum*) were calculated by an exponential function (Harley et al. 1992; Bernacchi et al. 2001; Long and Bernacchi 2003; Sharkey et al. 2007). The values of Rubisco specificity factor were 23.95 µmol $mol^{-1}$ for *Cypripedium* species and 32.21 µmol $mol^{-1}$ for *Paphiopedilum* species.

The value for chloroplast $CO_2$ concentration ($C_c$) was estimated by the following equation (Harley et al. 1992; Yamori et al. 2011):

$$C_c = C_i - \frac{A_N}{g_m}.$$

## Analysis of quantitative photosynthetic limitations

According to the method proposed by Grassi and Magnani (2005), the quantitative limitations on photosynthesis can be partitioned into stomatal conductance, mesophyll conductance, and biochemical capacity, i.e., $L_s + L_{mc} + L_b = 1$. Thus, the relative importance of stomatal diffusion, mesophyll diffusion, and photosynthetic biochemistry to the photosynthetic potential of each species was calculated as follows:

$$L_s = \frac{g_{tot}/g_s \cdot \partial A_N/\partial C_c}{g_{tot} + \partial A_N/\partial C_c},$$

$$L_{mc} = \frac{g_{tot}/g_m \cdot \partial A_N/\partial C_c}{g_{tot} + \partial A_N/\partial C_c},$$

$$L_b = \frac{g_{tot}}{g_{tot} + \partial A_N/\partial C_c},$$

where $g_{tot}$ is the total conductance of $CO_2$ from ambient air to carboxylation sites ($1/g_{tot} = 1/g_s + 1/g_m$) (Grassi and Magnani 2005). The photosynthetic limitation was calculated using the values of $A_N$ and $C_c$ at the ambient $CO_2$ concentration.

Further, we have calculated the limitations of the two biochemical processes (RuBP carboxylation or RuBP regeneration) on photosynthesis (Yamori et al. 2011). Chloroplast $CO_2$ concentration at which the transition from Rubisco to RuBP regeneration limitation occurs ($C_{transition}$) was calculated as

$$C_{transition} = \frac{K_c(1 + O/K_o)J_{max}/4V_{c,max} - 2\Gamma^*}{1 - J_{max}/4V_{c,max}},$$

where $O$ and $J_{max}$ are the intercellular $O_2$ concentration and the maximum rate of electron transport, respectively.

## Leaf anatomical traits

After the gas exchange parameters were examined, the middle parts of the same leaves used in those measurements were fixed in FAA (95% ethanol:distilled water:formaldehyde:glacial acetic acid, 10:7:2:1, v/v/v/v) for at least 24 h. These samples were cleaned with water prior to anatomical analysis. Transverse sections (18–40 μm) were made with a Microtome Cryostat (CM3050S; Leica, Germany) and then examined and photographed with a light microscope (U-CMAD3; Olympus Inc., Tokyo, Japan).

For further investigation, 1 × 1 mm pieces were excised from the portion of the leaf that was enclosed in the chamber. Those pieces were quickly infiltrated in the fixative 2.5% glutaraldehyde for at least 12 h and then post-fixed in 1% osmic acid for 2 h before being further dehydrated in an ethanol and acetone series. After the samples were embedded in LR White resin for 1 h, the cross sections (40 nm) were obtained with an ultramicrotome (Leica-R) and then stained with uranyl acetate and lead citrate. The ultrathin sections were viewed at the magnifications of ×1800 to ×40,000 by a JEOL JEM-1011 transmission electron microscope (JEOL Ltd. Tokyo, Japan) and photographed with an Olympus-SIS Megaview digital camera (Olympus Soft Imaging Solutions GmbH, Münster, Germany).

The images were used for determining the following parameters, using the ImageJ software package: leaf thickness (LT), mesophyll layer thickness (MT), adaxial and abaxial cuticle thicknesses ($CT_{ad}$ and $CT_{ab}$), adaxial and abaxial epidermis thicknesses vertically ($ET_{ad}$ and $ET_{ab}$), mesophyll cell length and width, chloroplast thickness ($T_{chlor}$), cell wall thickness ($T_{cw}$), total length of mesophyll cell perimeter facing the intercellular airspace ($L_{mes}$), and total length of chloroplast perimeter facing the intercellular airspace ($L_c$). Afterward, the mesophyll surface area exposed to intercellular airspace per unit leaf area ($S_{mes}/S$) and chloroplast surface area exposed to intercellular airspace per unit of leaf area ($S_c/S$) were calculated by applying the method of Tosens et al. (2012):

$$S_{mes}/S = \frac{L_{mes}}{W}\gamma,$$

$$S_c/S = \frac{L_c}{L_{mes}} S_{mes}/S,$$

where $W$ is the width of the sections measured and $\gamma$ is the curvature correction factor for each species, calculated as described by Thain (1983).

The fraction of intercellular airspace ($f_{ias}$) was determined as

$$f_{ias} = 1 - \frac{\sum S_s}{MT \cdot W},$$

where $\sum S_s$ is the sum of cross-sectional areas for mesophyll cells.

For a given section, all parameters were determined from at least eight fields of view, and at least five sections per species were analyzed.

### Leaf morphology

The abaxial epidermis from the middle part of a mature leaf was coated with a thin layer of colorless, transparent nail polish. After the polish dried, the film was gently torn away from the leaf surface with tweezers. These films were mounted on a microscope slide and images were taken with the light microscope. Randomly selected images (40 per species) were used to obtain the stomatal number and stomatal density (SD). Stomatal length (SL) and width (SW), referring to the length and width of the guard cells, were measured for 80 stomata, from which the stomatal aperture area (SA) could then be calculated as $1/4 \times \pi \times SL \times SW$ (James and Bell 2001). Pore depths were determined by examining those transverse sections (Lawson et al. 1998).

Leaf areas of the mature leaves used for monitoring gas exchange were measured with a leaf portable area meter (LI-3000A; Li-Cor). Afterward, the samples were oven-dried at 80 °C to a constant weight. The leaf dry mass was then weighed on a Mettler-Toledo analytical balance (ME 204; China) so that leaf dry mass per unit area (LMA) could be calculated. Then the leaf total nitrogen content ($N_{mass}$ and $N_{area}$) was measured using an elemental analyzer (Elementar Analysensysteme GmbH, Vario EL III, Hanau, Germany). And the photosynthetic nitrogen use efficiency (PNUE) was determined as

$$\mathrm{PNUE} = \frac{A_N}{N_{\mathrm{area}}},$$

where $A_N$ is the maximum photosynthetic rate at 380 μmol $mol^{-1}$ $CO_2$ concentration and $N_{area}$ is the leaf nitrogen content per unit area.

### Statistical analysis

Statistical analyses were performed with the IBM SPSS 21.0 software package (SPSS Inc., Chicago, IL, USA). Differences in leaf anatomical traits, photosynthetic parameters, and biochemical traits among species were determined by one-way ANOVA and Tukey's multiple comparison tests. A Pearson correlation analysis was used to evaluate the associations between parameters. Graphic images were produced using the Sigma Plot 10.0 package (Systat Software Inc., Richmond, CA, USA).

## Results

### Leaf morphologies and anatomies of *Cypripedium* and *Paphiopedilum*

Most of the leaf morphological and anatomical characteristics differed significantly between our selected species of *Cypripedium* and *Paphiopedilum* (Table 1, Appendix S2). Compared with *Cypripedium, Paphiopedilum* species had thicker leaves (LT = 1062 ± 85 μm) due to their larger adaxial epidermis cells ($E_{ad}$) and mesophyll thickness (MT). The values for $ET_{ad}$ and MT of *Paphiopedilum* were sixfold and threefold higher, respectively, than that for *Cypripedium*. Stomatal density (SD) and substomatal cavity area ($A_{sc}$) did

**Table 1** Differences in leaf anatomical and photosynthetic characteristics among *Cypripedium* and *Paphiopedilum* species based on *t* tests of independent samples

| Parameter | *Cypripedium* | *Paphiopedilum* | *P* value |
|---|---|---|---|
| LT (μm) | 292.7 ± 10.9 | **1062 ± 85** | 0.001 |
| $CT_{ad}$ (μm) | – | 21.3 ± 0.2 | – |
| $CT_{ab}$ (μm) | – | 12.6 ± 1.4 | – |
| $ET_{ad}$ (μm) | 48.9 ± 1.2 | **298.4 ± 71.1** | 0.025 |
| $ET_{ab}$ (μm) | 43.4 ± 0.6 | **72.6 ± 2.0** | 0.000 |
| MT (μm) | 199.2 ± 12.8 | **653.8 ± 70.7** | 0.003 |
| SD ($mm^{-2}$) | 32.9 ± 2.5 | **35.8 ± 5.8** | 0.665 |
| $A_s$ ($\mu m^2$) | **3386 ± 357** | 1549 ± 179 | 0.010 |
| PD (μm) | 26.7 ± 0.9 | **43.8 ± 1.1** | 0.000 |
| $A_{sc}$ ($\mu m^2$) | 2751 ± 513 | **2941 ± 460** | 0.796 |
| SCD (μm) | 41.2 ± 2.6 | **60.8 ± 4.4** | 0.018 |
| $T_{cw}$ (μm) | 0.45 ± 0.03 | **1.15 ± 0.20** | 0.072 |
| $S_{mes}/S$ ($m^2$ $m^{-2}$) | **6.45 ± 0.09** | 3.85 ± 0.26 | 0.001 |
| $S_c/S$ ($m^2$ $m^{-2}$) | **3.98 ± 0.11** | 1.99 ± 0.10 | 0.000 |
| $S_c/S_{mes}$ | **0.62 ± 0.02** | 0.52 ± 0.04 | 0.066 |
| $f_{ias}$ (%) | **27.1 ± 1.4** | 21.7 ± 1.3 | 0.046 |
| LMA (g $m^{-2}$) | 47.4 ± 1.4 | **151.5 ± 15.6** | 0.003 |
| $N_{mass}$ (%) | **2.53 ± 0.04** | 1.26 ± 0.07 | 0.001 |
| $N_{area}$ (g·$m^{-2}$) | 1.20 ± 0.05 | **1.90 ± 0.14** | 0.011 |
| PNUE (μmol $s^{-1}$ $CO_2$ $g^{-1}$ N) | **7.68 ± 0.89** | 1.50 ± 0.28 | 0.013 |
| $A_N$ (μmol $CO_2$ $m^{-2}$ $s^{-1}$) | **9.15 ± 0.77** | 2.77 ± 0.44 | 0.002 |
| $g_s$ (mol $CO_2$ $m^{-2}$ $s^{-1}$) | **0.22 ± 0.03** | 0.04 ± 0.01 | 0.003 |
| $g_m$ (mol $CO_2$ $m^{-2}$ $s^{-1}$) | **0.05 ± 0.00** | 0.01 ± 0.00 | 0.001 |
| $R_d$ (μmol $CO_2$ $m^{-2}$ $s^{-1}$) | −1.17 ± 0.26 | **−0.89 ± 0.05** | 0.387 |
| $V_{c,max}$ (μmol $CO_2$ $m^{-2}$ $s^{-1}$) | **34.6 ± 3.4** | 33.4 ± 6.8 | 0.883 |
| $C_i$ (μmol $mol^{-1}$) | **298.6 ± 2.1** | 258.8 ± 7.9 | 0.008 |
| $C_c$ (μmol $mol^{-1}$) | **108.2 ± 4.5** | 72.1 ± 9.7 | 0.028 |
| ETR (μmol $m^{-2}$ $s^{-1}$) | **85.8 ± 6.5** | 38.2 ± 2.2 | 0.002 |

Mean values ± SE (n = 3). *P* values indicate significant difference between species based on independent *t* test for each feature. Values in bold indicate the maximum value

not differ between the two genera. However, pore depth (PD) and substomatal cavity depth (SCD) were significantly larger for *Paphiopedilum* than for *Cypripedium*, while the area of individual stomata ($A_s$) was 2.2-fold higher.

Leaf anatomical traits were significantly different between genera (Table 1, Appendix S2, Figs. 1, 2). For example, the cell wall thickness ($T_{cw}$) was approximately 2.6-fold higher for *Paphiopedilum* than for *Cypripedium*, whereas the values calculated for the surface of mesophyll cells ($S_{mes}/S$) and the chloroplast ($S_c/S$) intercellular airspaces per leaf area were much larger for *Cypripedium* than for *Paphiopedilum*. Although the proportion of exposed chloroplast to mesophyll surface areas ($S_c/S_{mes}$) was 62% for *Cypripedium* but 52% for *Paphiopedilum*, no significant difference between genera was found for the intercellular airspaces ($f_{ias}$).

The leaf N content ($N_{mass}$) of *Cypripedium* was about twofold higher than that of *Paphiopedilum*. Conversely, the value of $N_{area}$ was $1.20 \pm 0.05$ g $m^{-2}$ for *Cypripedium*, but $1.90 \pm 0.14$ g $m^{-2}$ for *Paphiopedilum*. In addition, there were obvious differences in leaf dry mass per unit area (LMA) and photosynthetic nitrogen use efficiency (PNUE) between *Cypripedium* ($47.4 \pm 1.4$ g $m^{-2}$ and $7.68 \pm 0.89$ μmol $s^{-1}$ $CO_2$ $g^{-1}$ N, respectively) and *Paphiopedilum* ($151.5 \pm 15.6$ g $m^{-2}$ and $1.50 \pm 0.28$ μmol $s^{-1}$ $CO_2$ $g^{-1}$ N, respectively) (Table 1).

## Photosynthetic performances of *Cypripedium* and *Paphiopedilum*

At ambient $CO_2$, these six species differed greatly in their photosynthetic capacities (Table 1; Fig. 3, Appendix S3), with the net $CO_2$ assimilation rate being approximately 3.3-fold higher for members within *Cypripedium*. In particular, the $A_N$ values range from 10.4 μmol $CO_2$ $m^{-2}$ $s^{-1}$ for *C. flavum* down to only 1.94 μmol $CO_2$ $m^{-2}$ $s^{-1}$ for *P. dianthum* (Fig. 3). Similarly, the electron transport rate (ETR) was approximately 2.2-fold higher for *Cypripedium* (Fig. 4b). However, the maximum carboxylation rate ($V_{c,max}$) did not differ significantly between genera. Stomatal conductance was much higher for *Cypripedium* and the value of mesophyll conductance was approximately fivefold higher in that genus. Finally, mean values calculated for the substomatal

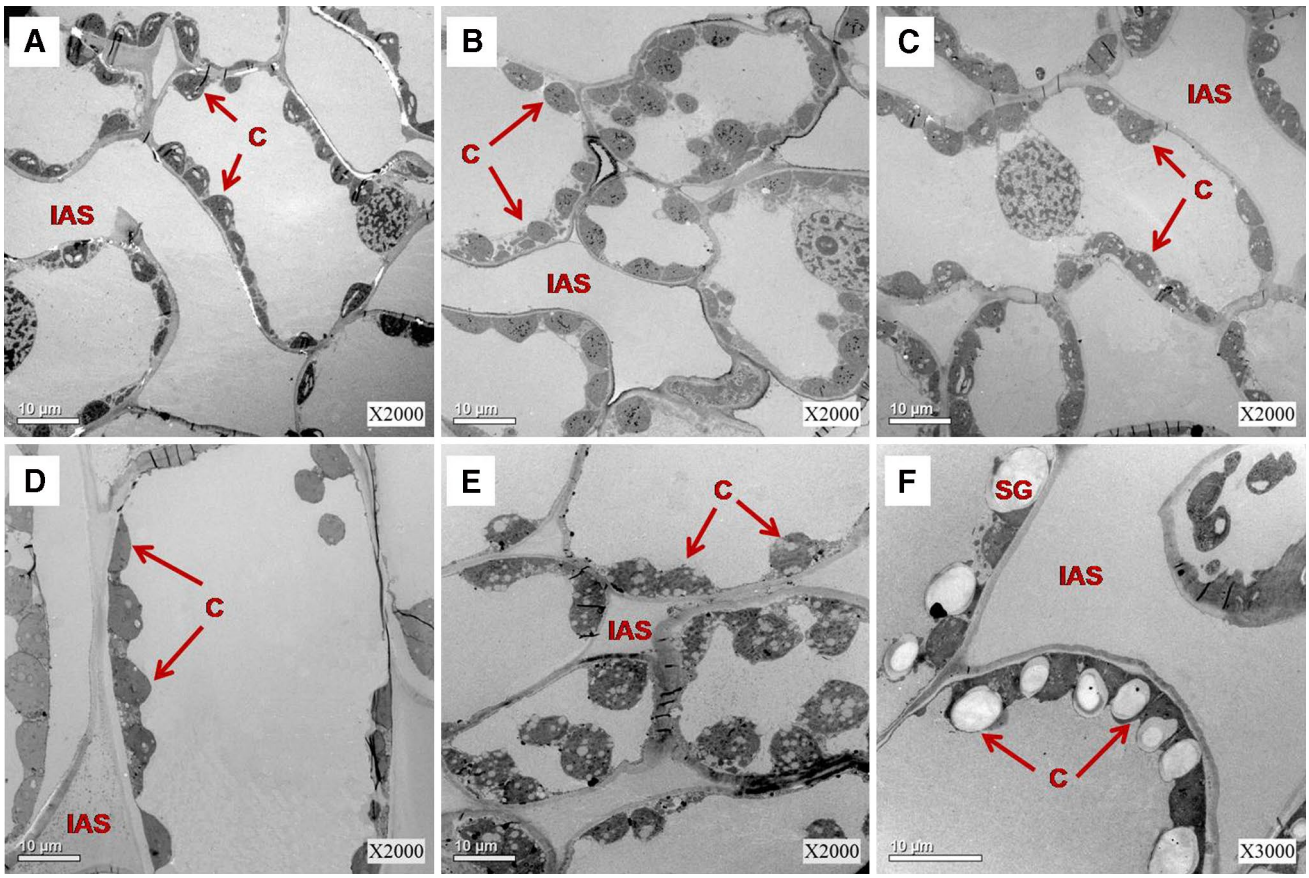


**Fig. 1** Transmission electron micrographs of transverse sections from adaxial mesophyll cells of *Cypripedium* and *Paphiopedilum*: **a** *C. flavum*, **b** *C. tibeticum*, **c** *C. yunnanense*, **d** *P. armeniacum*, **e** *P. micranthum*, and **f** *P. dianthum*. *C* chloroplast, *IAS* intercellular airspace, *SG* starch grains

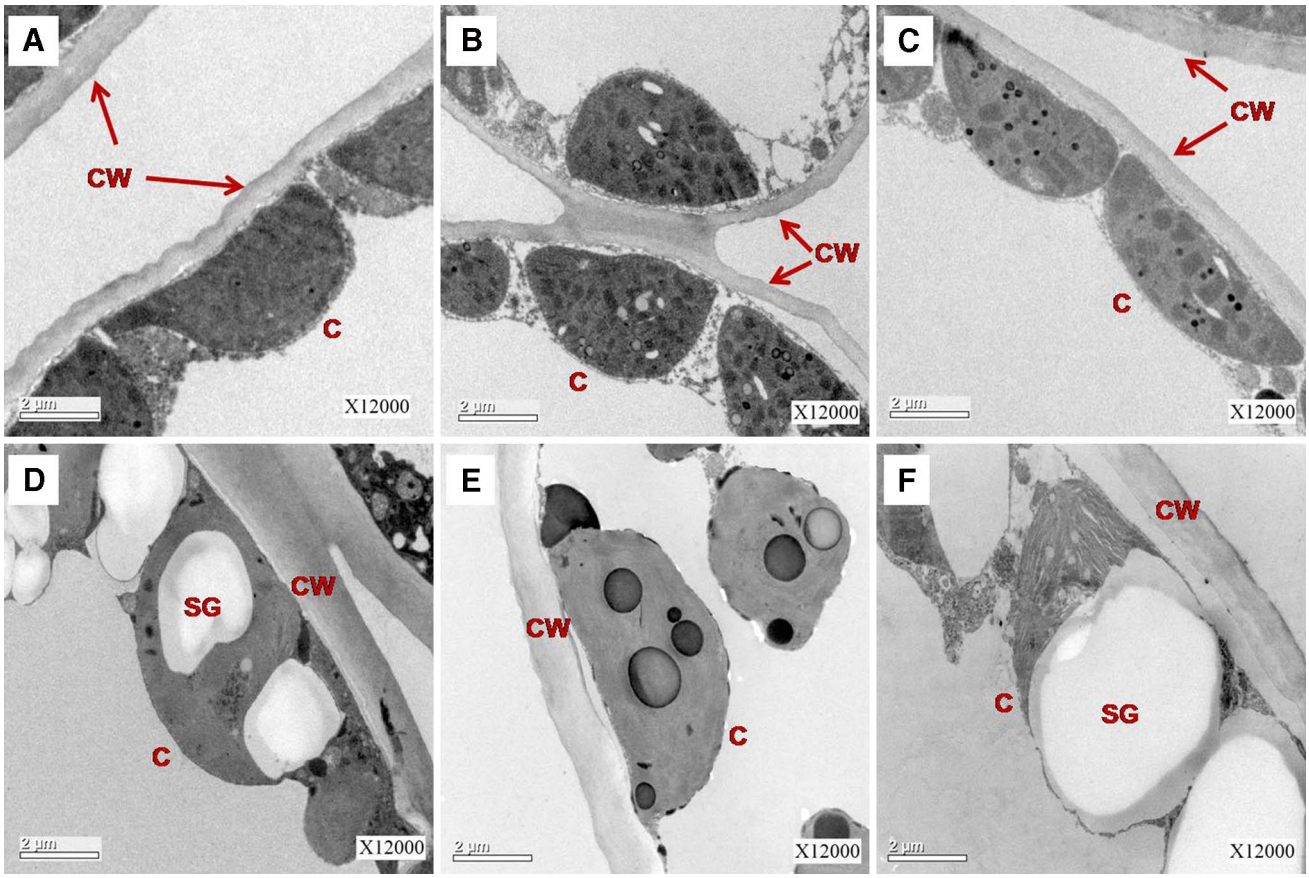


**Fig. 2** Transmission electron micrographs of transverse sections from cell walls of *Cypripedium* and *Paphiopedilum*: **a** *C. flavum*, **b** *C. tibeticum*, **c** *C. yunnanense*, **d** *P. armeniacum*, **e** *P. micranthum*, and **f** *P. dianthum. CW* cell wall, *C* chloroplast, *SG* starch grains

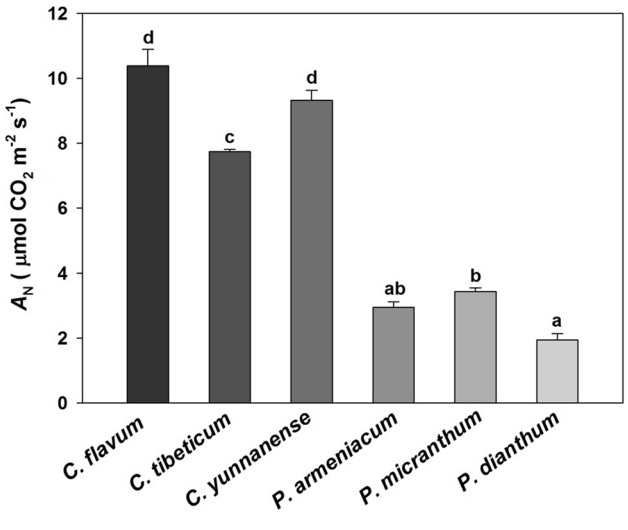


**Fig. 3** Light-saturated rate of $CO_2$ assimilation at 380 μmol $mol^{-1}$ $CO_2$ concentration ($A_N$) for six species from *Cypripedium* and *Paphiopedilum*. Values are means ± SE (n = 5)

and chloroplastic $CO_2$ concentrations were slightly higher in species of *Cypripedium*.

## Correlations between photosynthesis and leaf morphology and anatomy

Across species, several significant correlations were found between leaf structural traits, diffusional conductance, and photosynthetic rates (Figs. 5, 6, and Appendix S4). For example, $A_N$ was strongly and positively correlated with $g_s$ ($r = 0.997$; Fig. 5a) and $g_m$ ($r = 0.996$; Fig. 6a). In addition, $A_N$ was significantly associated with leaf morphological and anatomical traits. For example, it was correlated negatively with LT, $ET_{ad}$, $ET_{ab}$, MT, PD, SCD, and LMA, but positively with $A_s$, $S_{mes}/S$, and $S_c/S$. We also found that $g_s$ was strongly correlated with $A_s$ and PD (r = 0.95 and − 0.96, respectively), and $g_m$ was strongly correlated with $S_{mes}/S$, $S_c/S$, and $T_{cw}$ ($r = 0.99$, 0.98, and − 0.81, respectively). In addition, $g_s$ was negatively related to LT, $ET_{ab}$, and LMA, while $g_m$ had a negative correlation with LT, MT, and LMA.

We conducted a photosynthetic quantitative limitation analysis to examine the relative impacts of stomatal,

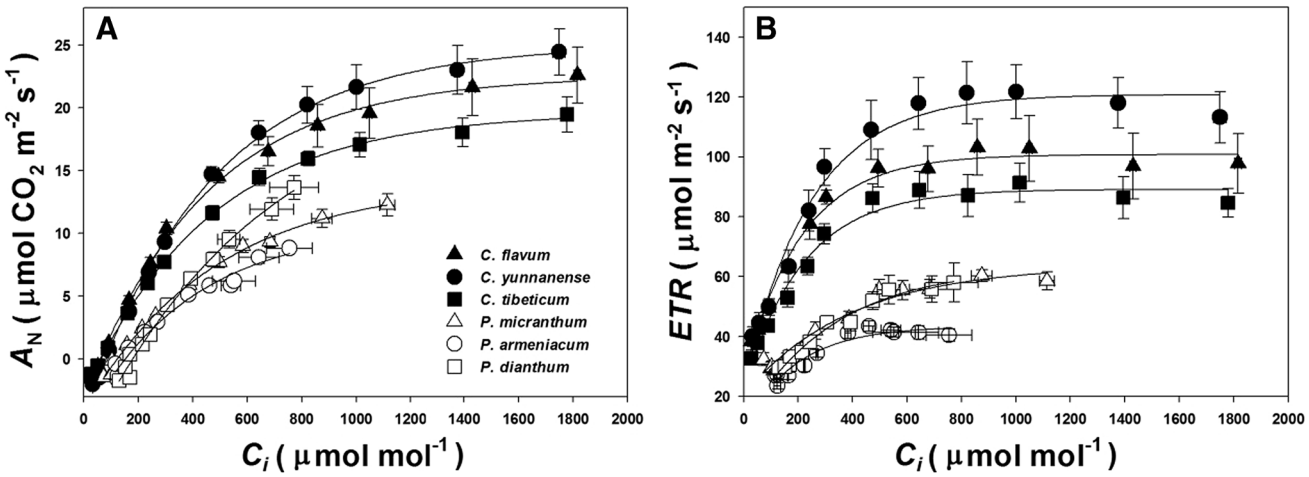


**Fig. 4** Response of $CO_2$ assimilation rate ($A_N$) (**a**) and electron transport rate (ETR) (**b**) to incident intercellular $CO_2$ concentration ($C_i$) in *Cypripedium* (black) and *Paphiopedilum* (white). Values are means ± SE (n = 5)

mesophyll conductance, and biochemical limitations on the photosynthetic potential of two genera (Fig. 7). Among those three, $L_{mc}$ had the greatest influence on *Cypripedium* (55.9% of the total) and *Paphiopedilum* (59.7%), while $L_s$ had the least impact, i.e., 12.3% for *Cypripedium* and 19.8% for *Paphiopedilum*. Finally, the total diffusional limitation ($L_s + L_{mc}$) on photosynthesis was larger for *Paphiopedilum* (79.5%) than for *Cypripedium* (68.2%). We also analyzed the limitations of two biochemical processes on photosynthesis and found that $C_c$ for $A_{380}$ ($A_N$ at 380 mmol $mol^{-1}$ $CO_2$ concentrations, Table 1) was less than the $C_{transition}$ (197.2 µmol $mol^{-1}$ for *Paphiopedilum*, but 116.9 µmol $mol^{-1}$ for *Cypripedium*), indicating that $CO_2$ assimilation was limited by RuBP carboxylation in both genera.

## Discussion

We believe that this study is the first report to explore why orchids have low photosynthetic potential by using an integrated approach. Using six species of *Cypripedium* and *Paphiopedilum*, we demonstrated that leaf anatomy and morphology play key roles in regulating leaf diffusional conductance, thereby affecting photosynthetic performance. Our results indicated that many of the leaf morphological, anatomical, and physiological traits measured here differed significantly between these closely related genera. Compared with *Cypripedium, Paphiopedilum* species had much thicker leaves and cell walls, expanded adaxial epidermal cells, very large mesophyll cells, greater pore depth, and higher leaf dry mass per unit area, but smaller area for the stomatal apparatus, less surface area for mesophyll cells, and reduced intercellular airspaces in the chloroplasts per leaf area. Meanwhile, *Cypripedium* had a reduced $T_{cw}$ and larger $S_{mes}/S$ and $S_c/S$, but significantly higher stomatal conductance, mesophyll conductance, leaf nitrogen content, photosynthetic nitrogen use efficiency, electron transport rate, and photosynthetic capacity. Some of these findings are in accordance with the results reported previously (Chang et al. 2011; Guan et al. 2011). These obvious differences in leaf traits between the closely related genera reflect the adaptation to their habitats. The natural growth conditions of *Cypripedium* are usually characterized by nutrient-rich soils and high soil moisture content during the growing season. Conversely, the natural habitats of *Paphiopedilum* in the karst limestone area are accompanied by low availability of substrates for storing water and nutrients. *Paphiopedilum* has features which may enable growth in moderate xerophytic conditions due to periodic shortages of water; this includes large epidermal cells, a thicker layer of mesophyll cells, a thicker cuticle, small stomata, high leaf dry mass per unit area, a relatively low leaf N content, and photosynthetic nitrogen use efficiency. These features could prevent excessive transpiration, support storage of water, with investment of more resources (C and N) into the construction and maintenance of leaves and less into the photosynthetic apparatus. We believe that the lower photosynthetic capacity of *Paphiopedilum* was caused by the lower values of $N_{mass}$, PNUE, ETR, $g_s$, and $g_m$ compared with *Cypripedium*. And all of these observations provide evidence that differences among species in their leaf structures and photosynthetic performances are indicative of their abilities to adapt to their environments.

Our results showed that leaf morphological and anatomical structures have crucial roles in regulating diffusional resistance and photosynthetic performance for *Cypripedium* and *Paphiopedilum*. This may occur because such traits control the diffusion of gas between the outside and the inside

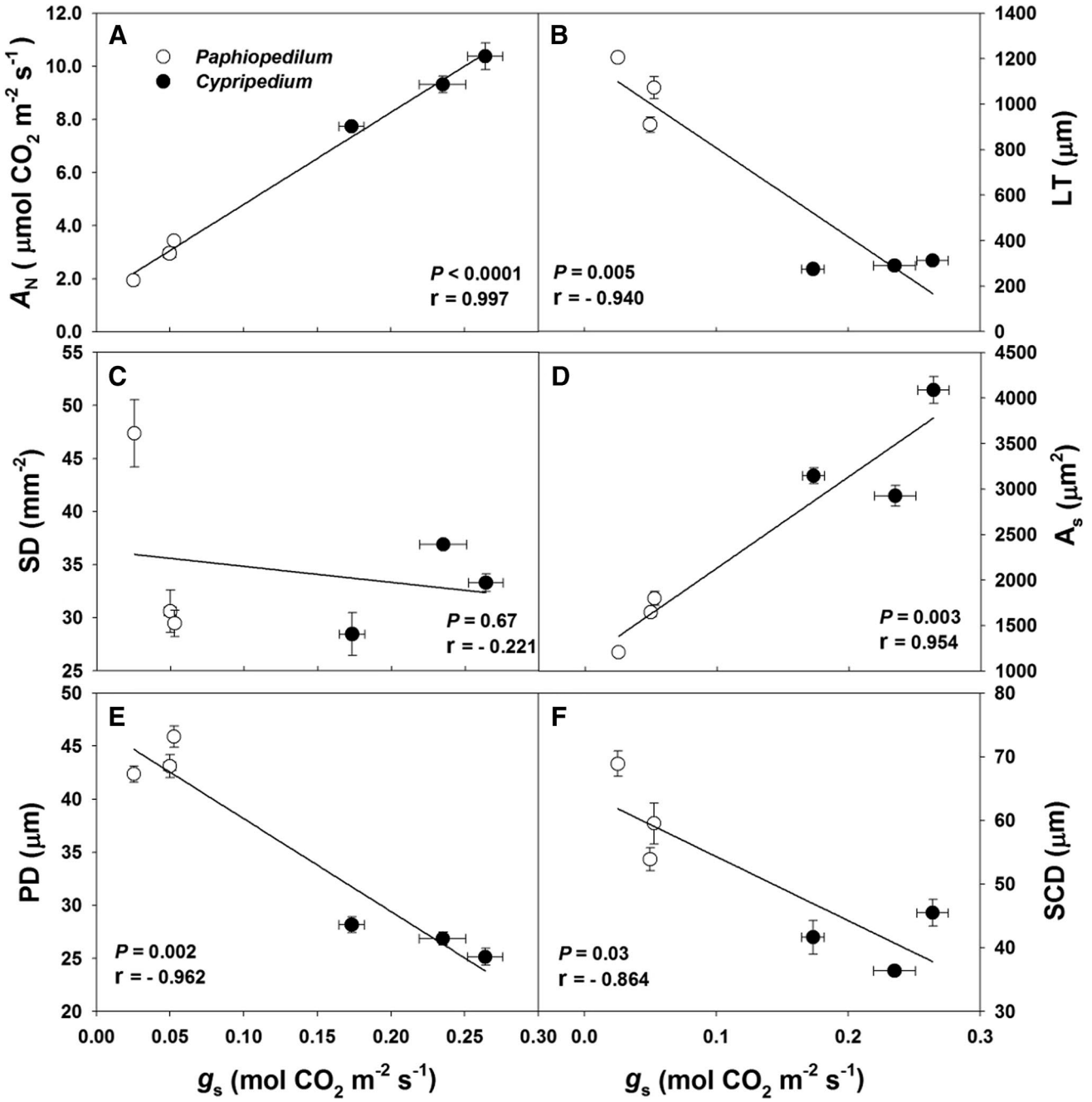


**Fig. 5** Correlations between $CO_2$ assimilation rate, stomatal conductance, and leaf structure: **a** stomatal conductance ($g_s$) versus $CO_2$ assimilation rate ($A_N$); **b** $g_s$ versus leaf thickness (LT); **c** $g_s$ versus stomatal density (SD); **d** $g_s$ versus stomatal apparatus area ($A_s$); **e** $g_s$ versus pore depth (PD); and **f** $g_s$ versus substomatal cavity depth (SCD). Values are means ± SE ($n = 5$) for *Cypripedium* (black dots) and *Paphiopedilum* (white dots)

of the leaf (Niinemets and Sack 2006; Boyer 2015). Stomata are keys in determining internal $CO_2$ concentrations (Farquhar and Sharkey 1982; Araujo et al. 2011; Taylor et al. 2012). We found that the $g_s$ value was lower in *Paphiopedilum* than in *Cypripedium*, and $g_s$ was positively correlated with $A_N$ across the six species. This relationship is in accordance with the theoretical basis of the Ball–Berry model (Ball et al. 1987). Our analysis of photosynthetic limitations confirmed that stomatal factors were stronger in *Paphiopedilum*. A positive correlation between maximum $A_N$ and $g_s$ has been observed in other species and various habitats (Patakas et al. 2003; Gago et al. 2013, 2016). The lower $g_s$ of *Paphiopedilum* means that this genus displays greater stomatal resistance that reduces the concentration

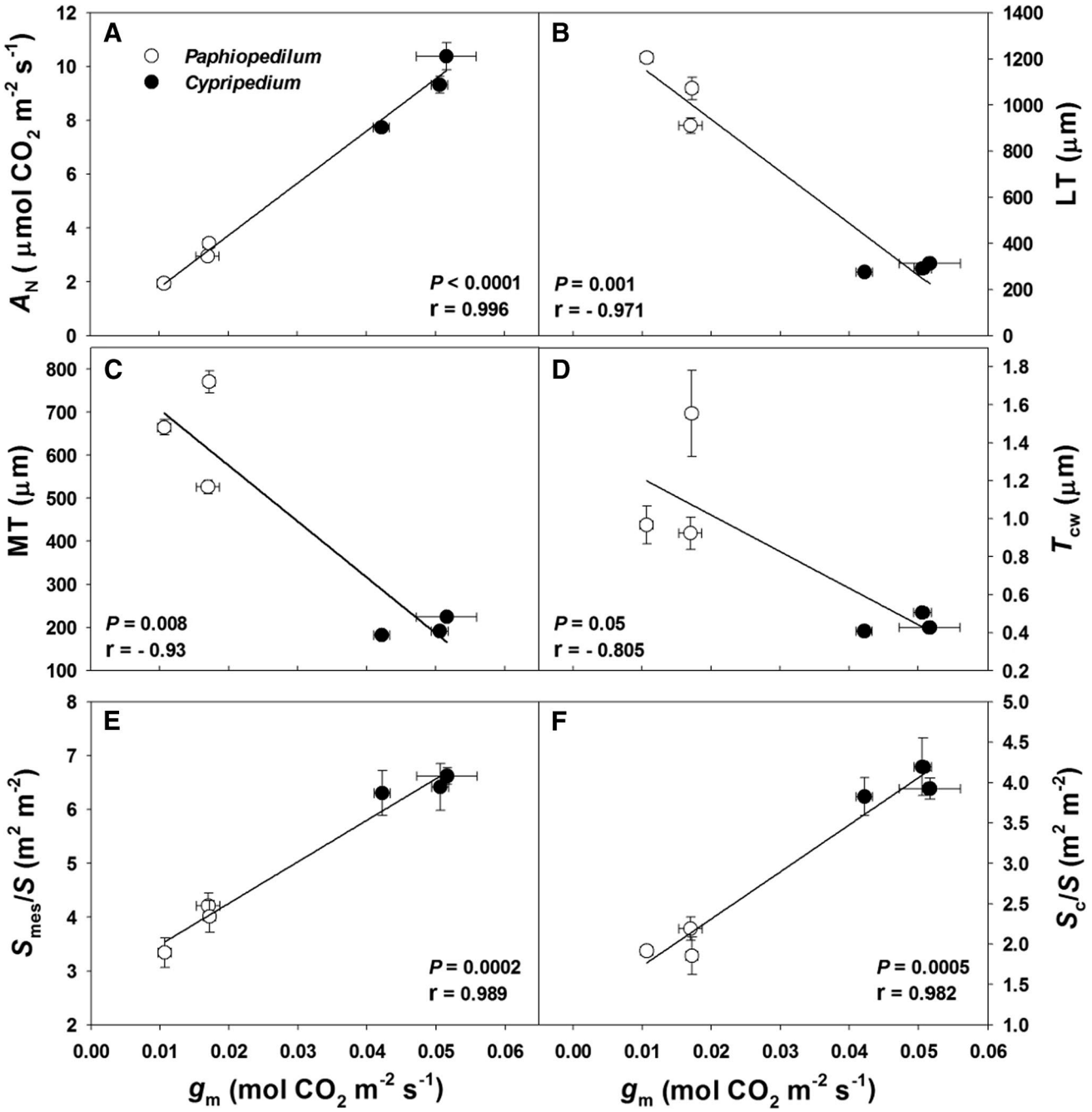


**Fig. 6** Correlations between $CO_2$ assimilation rate, mesophyll conductance, and leaf structure: **a** mesophyll conductance ($g_m$) versus $CO_2$ assimilation rate ($A_N$); **b** $g_m$ versus leaf thickness (LT); **c** $g_m$ versus mesophyll layer thickness (MT); **d** $g_m$ versus cell wall thickness ($T_{cw}$); **e** $g_m$ versus surface area of mesophyll cells exposed to airspace per unit of leaf area ($S_{mes}/S$); and **f** $g_m$ versus chloroplast surface area exposed to intercellular airspace per unit of leaf area ($S_c/S$). Values are means ± SE ($n = 5$) for *Cypripedium* (black dots) and *Paphiopedilum* (white dots)

of $CO_2$ in the chloroplasts and leads to a lower photosynthetic rate. It is commonly thought that $g_s$ is mainly affected by both stomatal density/size and whether the stomata are open (Franks and Beerling 2009; Ocheltree et al. 2012; de Boer et al. 2016). In contrast, our results indicated that $g_s$ is strongly linked to $A_s$, PD, SCD, and LMA, but is not significantly correlated with SD. Therefore, we might conclude that $A_s$ and PD are the most conspicuous stomatal features that determine the degree of stomatal opening and the distance that $CO_2$ diffuses through the stomata, respectively, thereby jointly affecting the leaf internal $CO_2$ concentration. Some previous studies have also shown that $A_s$

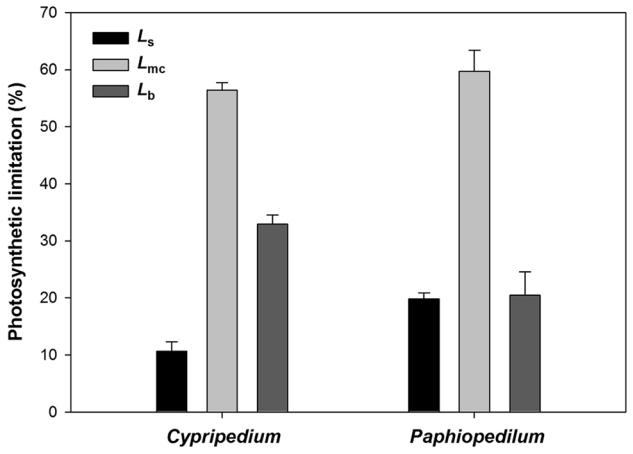


**Fig. 7** Relative stomatal ($L_s$), mesophyll conductance ($L_{mc}$), and biochemical ($L_b$) limitations to photosynthesis in *Cypripedium* and *Paphiopedilum*

is closely correlated with $g_s$ (Giuliani et al. 2013; Brodribb et al. 2016). Overall, our results suggest that stomatal area and pore depth, rather than stomatal density, are the most important factors that influence $g_s$ in our selected species.

Mesophyll conductance plays an important role in determining the $CO_2$ concentration at the sites of carboxylation inside the chloroplasts. Other researchers have also demonstrated that $g_m$ is an important factor for the limitation of photosynthesis (Flexas et al. 2008, 2012; Sagardoy et al. 2010) and is positively correlated with the photosynthetic rate (Loreto et al. 2003; Singsaas et al. 2004; Grassi and Magnani 2005; Warren and Adams 2006). For example, $g_m$ is responsible for the lower photosynthetic capacity in ferns when compared with angiosperms (Carriqui et al. 2015). We also noted the role that $g_m$ has in controlling photosynthesis in our tested species and found that *Paphiopedilum* has a higher mesophyll limitation than does *Cypripedium*. The positive relationship between photosynthetic rate and mesophyll conductance for *Cypripedium* and *Paphiopedilum* growing in their natural distribution areas was also confirmed by our study (Appendix S5) and a previous study (Chang et al. 2011), respectively. This has also been revealed elsewhere. For example, Tomas et al. (2013) reported that $g_m$ is highly correlated with $S_c/S$ and $T_{cw}$ in 15 fern species, but that the effects of leaf anatomical features on $g_m$ vary among species. For plants with mesophytic leaves, membrane permeability, the cytosol, and stromal conductance dictate $g_m$, while $T_{cw}$ is the most important limitation for plants with sclerophytic leaves. In fact, some models have estimated that approximately 25–50% of the variability in $g_m$ can be explained by differences in cell wall thickness (Evans et al. 2009; Tosens et al. 2012). However, other researchers have suggested that the majority of $g_m$ variation is due to the combination of three parameters: $S_{mes}/S$, $S_c/S$, and $T_{cw}$ (Fini et al. 2016; Xiong et al. 2016). Our evaluation of six orchid species indicated that $g_m$ increased linearly with $S_{mes}/S$ and $S_c/S$ but decreased linearly with $T_{cw}$. We were surprised to learn that $g_m$ was also related to LT, MT, and LMA. While leaf thickness and cell wall thickness affect the length of the $CO_2$ diffusion path, $S_{mes}/S$ and $S_c/S$ determine the number of photosynthetic carboxylation sites adjacent to the intercellular airspace (Flexas et al. 2012; Tosens et al. 2012). These relationships collectively demonstrate that the leaf anatomical structure is associated with the internal diffusion of $CO_2$ conductance and photosynthetic performances of species within *Paphiopedilum* and *Cypripedium*.

In summary, the combination of stomatal, mesophyll, and biochemical factors help determine the photosynthetic potentials of *Paphiopedilum* and *Cypripedium*. However, photosynthetic capacity is more strongly influenced by diffusional limitations than by biochemical limitations. Mesophyll conductance plays a vital role in the performance of the six orchids tested here. Both stomatal apparatus area and pore depth are the key anatomical traits that affect stomatal conductance, while mesophyll conductance is modulated by the surface area of mesophyll cells exposed to intercellular airspace per unit of leaf area, the chloroplast surface area exposed to intercellular airspace per unit of leaf area, and cell wall thickness. Therefore, the lower photosynthetic rate in *Paphiopedilum* species can largely be explained by diffusional resistance, particularly internal resistance which is imposed by their unique leaf anatomy and morphology. These findings provided new insight into the evolution of leaf structures, photosynthetic physiology, and slow growth rates by orchids. However, the phenotypes of plants are a consequence of differences in their genotypes and response to their environments; thus, further studies on structural and biochemical differences between representative species in these genera growing in their natural habitats will be of interest.

**Acknowledgements** This work was financially supported by the National Natural Science Foundation of China (31670342, 31370362, 31400289, and 31670415) and the National Key Project of the Ministry of Science and Technology of China (2015BAD10B03).

## References

Araujo WL, Nunes-Nesi A, Osorio S, Usadel B, Fuentes D, Nagy R, Balbo I, Lehmann M, Studart-Witkowski C, Tohge T, Martinoia E, Jordana X, DaMatta FM, Fernie AR (2011) Antisense inhibition of the iron-sulphur subunit of succinate dehydrogenase enhances photosynthesis and growth in tomato via an organic acid-mediated effect on stomatal aperture. Plant Cell 23:600–627

Assmann SM, Zeiger E (1985) Stomatal responses to $CO_2$ in *Paphiopedilum* and *Phragmipedium*-role of the guard-cell chloroplast. Plant Physiol 77:461–464

Ball JT, Woodrow IE, Berry JA (1987) A model predicting stomatal conductance and its contribution to the control of photosynthesis

under different environmental conditions. In: Biggens JE (ed) Progress in photosynthesis research. Martinus Nijhoff Publishers, Dordrecht, pp 221–224

Bernacchi CJ, Singsaas EL, Pimentel C, Portis AR, Long SP (2001) Improved temperature response functions for models of Rubisco-limited photosynthesis. Plant Cell Environ 24:253–259

Boyer JS (2015) Turgor and the transport of $CO_2$ and water across the cuticle (epidermis) of leaves. J Exp Bot 66:2625–2633

Brodribb TJ, McAdam SA, Carins Murphy MR (2017) Xylem and stomata, coordinated through time and space. Plant Cell Environ 40:872–880

Cameron KM, Chase MW, Whitten WM, Kores PJ, Jarrell DC, Albert VA, Yukawa T, Hills HG, Goldman DH (1999) A phylogenetic analysis of the Orchidaceae: evidence from rbcL nucleotide sequences. Am J Bot 86:208–224

Carriqui M, Cabrera HM, Conesa MA, Coopman RE, Douthe C, Gago J, Galle A, Galmes J, Ribas-Carbo M, Tomas M, Flexas J (2015) Diffusional limitations explain the lower photosynthetic capacity of ferns as compared with angiosperms in a common garden study. Plant Cell Environ 38:448–460

Chang W, Zhang SB, Li SY, Hu H (2011) Ecophysiological significance of leaf traits in *Cypripedium* and *Paphiopedilum*. Physiol Plant 141:30–39

Christenhusz MJM, Byng JW (2016) The number of known plants species in the world and its annual increase. Phytotaxa 261:201–217

Cox AV, Pridgeon AM, Albert VA, Chase MW (1997) Phylogenetics of the slipper orchids (Cypripedioideae, Orchidaceae): nuclear rDNA ITS sequences. Plant Syst Evol 208:197–223

Crain BJ, Tremblay RL (2014) Do richness and rarity hotspots really matter for orchid conservation in light of anticipated habitat loss? Divers Distrib 20:652–662

de Boer HJ, Price CA, Wagner-Cremer F, Dekker SC, Franks PJ, Veneklaas EJ (2016) Optimal allocation of leaf epidermal area for gas exchange. New Phytol 210:1219–1228

Dressler RL (1993) Phylogeny and classification of the orchid family. Cambridge University Press, Cambridge

Dunbar-Co S, Sporck MJ, Sack L (2009) Leaf trait diversification and design in seven rare taxa of the Hawaiian *Plantago* radiation. Int J Plant Sci 170:61–75

Evans JR, von Caemmerer S (1996) Carbon dioxide diffusion inside leaves. Plant Physiol 110:339–346

Evans JR, Kaldenhoff R, Genty B, Terashima I (2009) Resistances along the $CO_2$ diffusion pathway inside leaves. J Exp Bot 60:2235–2248

Farquhar GD, Sharkey TD (1982) Stomatal conductance and photosynthesis. Annu Rev Plant Phys 33:317–345

Fini A, Loreto F, Tattini M, Giordano C, Ferrini F, Brunetti C, Centritto M (2016) Mesophyll conductance plays a central role in leaf functioning of Oleaceae species exposed to contrasting sunlight irradiance. Physiol Plant 157:54–68

Flexas J, Ribas-Carbo M, Hanson DT, Bota J, Otto B, Cifre J, McDowell N, Medrano H, Kaldenhoff R (2006) Tobacco aquaporin NtAQP1 is involved in mesophyll conductance to $CO_2$ in vivo. Plant J 48:427–439

Flexas J, Ribas-Carbo M, Diaz-Espejo A, Galmes J, Medrano H (2008) Mesophyll conductance to $CO_2$: current knowledge and future prospects. Plant Cell Environ 31:602–621

Flexas J, Barbour MM, Brendel O, Cabrera HM, Carriqui M, Diaz-Espejo A, Douthe C, Dreyer E, Ferrio JP, Gago J, Galle A, Galmes J, Kodama N, Medrano H, Niinemets U, Peguero-Pina JJ, Pou A, Ribas-Carbo M, Tomas M, Tosens T, Warren CR (2012) Mesophyll diffusion conductance to $CO_2$: an unappreciated central player in photosynthesis. Plant Sci 193:70–84

Flexas J, Carriqui M, Coopman RE, Gago J, Galmes J, Martorell S, Morales F, Diaz-Espejo A (2014) Stomatal and mesophyll conductances to $CO_2$ in different plant groups: Underrated factors for predicting leaf photosynthesis responses to climate change? Plant Sci 226:41–48

Franks PJ, Beerling DJ (2009) Maximum leaf conductance driven by $CO_2$ effects on stomatal size and density over geologic time. P Natl Acad Sci USA 106:10343–10347

Franks PJ, Farquhar GD (2007) The mechanical diversity of stomata and its significance in gas-exchange control. Plant Physiol 143:78–87

Gago J, Coopman RE, Cabrera HM, Hermida C, Molins A, Conesa MA, Galmes J, Ribas-Carbo M, Flexas J (2013) Photosynthesis limitations in three fern species. Physiol Plant 149:599–611

Gago J, Daloso DM, Figueroa CM, Flexas J, Fernie AR, Nikoloski Z (2016) Relationships of leaf net photosynthesis, stomatal conductance, and mesophyll conductance to primary metabolism: A multispecies meta-analysis approach. Plant Physiol 171:265–279

Giuliani R, Koteyeva N, Voznesenskaya E, Evans MA, Cousins AB, Edwards GE (2013) Coordination of leaf photosynthesis, transpiration, and structural traits in rice and wild relatives (genus *Oryza*). Plant Physiol 162:1632–1651

Grassi G, Magnani F (2005) Stomatal, mesophyll conductance and biochemical limitations to photosynthesis as affected by drought and leaf ontogeny in ash and oak trees. Plant Cell Environ 28:834–849

Guan ZJ (2010) Leaf traits of *Paphiopedilum* and *Cypripedium* in Orchidaceae. PhD thesis, Kunming Institute of Botany, Chinese Academy of Sciences, China

Guan ZJ, Zhang SB, Guan KY, Li SY, Hu H (2011) Leaf anatomical structures of *Paphiopedilum* and *Cypripedium* and their adaptive significance. J Plant Res 124:289–298

Han JM, Meng HF, Wang SY, Jiang CD, Liu F, Zhang WF, Zhang YL (2016) Variability of mesophyll conductance and its relationship with water use efficiency in cotton leaves under drought pretreatment. J Plant Physiol 194:61–71

Harley PC, Loreto F, Marco GD, Sharkey TD (1992) Theoretical considerations when estimating the mesophyll conductance to $CO_2$ flux by analysis of the response of photosynthesis to $CO_2$. Plant Physiol 98:1429–1436

Hew CS, Yong JWH (2004) The PHYSIOLOGY OF TROPICAL ORCHIDS IN RELATION TO THE INDUSTRY. World Scientific, Singapore

Holbrook NM, Putz FE (1996) From epiphyte to tree: differences in leaf structure and leaf water relations associated with the transition in growth form in eight species of hemiepiphytes. Plant Cell Environ 19:631–642

James SA, Bell DT (2001) Leaf morphological and anatomical characteristics of heteroblastic *Eucalyptus globulus* ssp. *globulus* (Myrtaceae). Aust J Bot 49:259–269

Kerbauy GB, Takahashi CA, Lopez AM, Matsumura AT, Hamachi L, Félix LM, Pereira PN, Freschi L, Mercier H (2012) Crassulacean acid metabolism in epiphytic orchids: current knowledge, future perspectives. In: Najafpour MM (ed) Applied Photosynthesis. InTech, Rijeka, pp 81–104

Laclau JP, Toutain F, M'Bou AT, Arnaud M, Joffre R, Ranger J (2004) The function of the superficial root mat in the biogeochemical cycles of nutrients in Congolese Eucalyptus plantations. Ann Bot 93:249–261

Lawson T, James W, Weyers J (1998) A surrogate measure of stomatal aperture. J Exp Bot 49:1397–1403

Long SP, Bernacchi CJ (2003) Gas exchange measurements, what can they tell us about the underlying limitations to photosynthesis? Procedures and sources of error. J Exp Bot 54:2393–2401

Loreto F, Centritto M, Chartzoulakis K (2003) Photosynthetic limitations in olive cultivars with different sensitivity to salt stress. Plant Cell Environ 26:595–601

Moreira ASFP., de Lemos JP, Zotz G, Isaias RMD (2009) Anatomy and photosynthetic parameters of roots and leaves of two

shade-adapted orchids, *Dichaea cogniauxiana* Shltr. and *Epidendrum secundum*. Jacq Flora 204:604–611

Muir CD, Hangarter RP, Moyle LC, Davis PA (2014) Morphological and anatomical determinants of mesophyll conductance in wild relatives of tomato (*Solanum* sect. *Lycopersicon*, sect. Lycopersicoides; Solanaceae). Plant Cell Environ 37:1415–1426

Niinemets Ü, Sack L (2006) Structural determinants of leaf light-harvesting capacity and photosynthetic potentials. Prog Bot 67:385–419

Niinemets Ü, Cescatti A, Rodeghiero M, Tosens T (2005) Leaf internal diffusion conductance limits photosynthesis more strongly in older leaves of Mediterranean evergreen broad-leaved species. Plant Cell Environ 28:1552–1566

Niinemets Ü, Diaz-Espejo A, Flexas J, Galmes J, Warren CR (2009) Role of mesophyll diffusion conductance in constraining potential photosynthetic productivity in the field. J Exp Bot 60:2249–2270

Obeso JR (2002) The cost of reproduction in plants. New Phytol 155:321–348

Ocheltree TW, Nippert JB, Prasad PVV (2012) Changes in stomatal conductance along grass blades reflect changes in leaf structure. Plant Cell Environ 35:1040–1049

Oguchi R, Hikosaka K, Hirose T (2003) Does the photosynthetic light-acclimation need change in leaf anatomy? Plant Cell Environ 26:505–512

Patakas A, Kofidis G, Bosabalidis AM (2003) The relationships between $CO_2$ transfer mesophyll resistance and photosynthetic efficiency in grapevine cultivars. Sci Hortic-Amsterdam 97:255–263

Peguero-Pina JJ, Flexas J, Galmes J, Niinemets Ü, Sancho-Knapik D, Barredo G, Villarroya D, Gil-Pelegrin E (2012) Leaf anatomical properties in relation to differences in mesophyll conductance to $CO_2$ and photosynthesis in two related Mediterranean *Abies* species. Plant Cell Environ 35:2121–2129

Peguero-Pina JJ, Siso S, Flexas J, Galmes J, Garcia-Nogales A, Niinemets Ü, Sancho-Knapik D, Saz MA, Gil-Pelegrin E (2017) Cell-level anatomical characteristics explain high mesophyll conductance and photosynthetic capacity in sclerophyllous Mediterranean oaks. New Phytol 214:585–596

Sagardoy R, Vazquez S, Florez-Sarasa ID, Albacete A, Ribas-Carbo M, Flexas J, Abadia J, Morales F (2010) Stomatal and mesophyll conductances to $CO_2$ are the main limitations to photosynthesis in sugar beet (*Beta vulgaris*) plants grown with excess zinc. New Phytol 187:145–158

Sawada S, Sato M, Kasai A, Yaochi D, Kameya Y, Matsumoto I, Kasai M (2003) Analysis of the feed-forward effects of sink activity on the photosynthetic source-sink balance in single-rooted sweet potato leaves. I. Activation of RuBPcase through the development of sinks. Plant Cell Physiol 44:190–197

Sharkey TD, Bernacchi CJ, Farquhar GD, Singsaas EL (2007) Fitting photosynthetic carbon dioxide response curves for $C_3$ leaves. Plant Cell Environ 30:1035–1040

Shefferson RP (2006) Survival costs of adult dormancy and the confounding influence of size in lady's slipper orchids, genus *Cypripedium*. Oikos 115:253–262

Singsaas EL, Ort DR, Delucia EH (2004) Elevated $CO_2$ effects on mesophyll conductance and its consequences for interpreting photosynthetic physiology. Plant Cell Environ 27:41–50

Taylor SH, Franks PJ, Hulme SP, Spriggs E, Christin PA, Edwards EJ, Woodward FI, Osborne CP (2012) Photosynthetic pathway and ecological adaptation explain stomatal trait diversity amongst grasses. New Phytol 193:387–396

Terashima I, Hanba YT, Tazoe Y, Vyas P, Yano S (2006) Irradiance and phenotype: comparative eco-development of sun and shade leaves in relation to photosynthetic $CO_2$ diffusion. J Exp Bot 57:343–354

Thain JF (1983) Curvature correlation factors in the measurements of cell surface areas in plant tissues. J Exp Bot 34:87–94

Tholen D, Zhu XG (2011) The mechanistic basis of internal conductance: a theoretical analysis of mesophyll cell photosynthesis and $CO_2$ diffusion. Plant Physiol 156:90–105

Tomas M, Flexas J, Copolovici L, Galmes J, Hallik L, Medrano H, Ribas-Carbo M, Tosens T, Vislap V, Niinemets U (2013) Importance of leaf anatomy in determining mesophyll diffusion conductance to $CO_2$ across species: quantitative limitations and scaling up by models. J Exp Bot 64:2269–2281

Tosens T, Niinemets Ü, Westoby M, Wright IJ (2012) Anatomical basis of variation in mesophyll resistance in eastern Australian sclerophylls: news of a long and winding path. J Exp Bot 63:5105–5119

Tosens T, Nishida K, Gago J, Coopman RE, Cabrera HM, Carriqui M, Laanisto L, Morales L, Nadal M, Rojas R, Talts E, Tomas M, Hanba Y, Niinemets Ü, Flexas J (2016) The photosynthetic capacity in 35 ferns and fern allies: mesophyll $CO_2$ diffusion as a key trait. New Phytol 209:1576–1590

von Caemmerer S (2000) Biochemical models of leaf photosynthesis. CSIRO Publishing, Collingwood

Warren CR, Adams MA (2006) Internal conductance does not scale with photosynthetic capacity: implications for carbon isotope discrimination and the economics of water and nitrogen use in photosynthesis. Plant Cell Environ 29:192–201

Xiong D, Flexas J, Yu T, Peng S, Huang J (2017) Leaf anatomy mediates coordination of leaf hydraulic conductance and mesophyll conductance to $CO_2$ in *Oryza*. New Phytol 213:572–583

Yamori W, Nagai T, Makino A (2011) The rate-limiting step for $CO_2$ assimilation at different temperatures is influenced by the leaf nitrogen content in several C3 crop species. Plant Cell Environ 34:764–777

Yamori W, Masumoto C, Fukayama H, Makino A (2012) Rubisco activase is a key regulator of non-steady-state photosynthesis at any leaf temperature and to a lesser extent of steady-state photosynthesis at high temperature. Plant J 71:871–880

Zhang SB, Hu H, Xu K, Li ZH (2006) Photosynthetic performances of five *Cypripedium* species after transplanting. Photosynthetica 44:425–432

Zhang SB, Guan Z, Chang W, Ning Y, Hu H (2010) Ecophysiological traits of *Paphiopedilum* and *Cypripedium*. Acta Hortic 878:37–42

Zhang SB, Guan ZJ, Sun M, Zhang JJ, Cao KF, Hu H (2012) Evolutionary association of stomatal traits with leaf vein density in *Paphiopedilum*, Orchidaceae. PLoS One 7:e40080

Zhang SB, Dai Y, Hao GY, Li JW, Fu XW, Zhang JL (2015) Differentiation of water-related traits in terrestrial and epiphytic *Cymbidium* species. Front Plant Sci 6:260